

## Development of a Coupled Tendon Driven Robot Hand

H.R. Choi, Y.T. Lee, J.H. Kim, W.K. Chung, and Y. Youm  
 Robotics Lab., Department of Mechanical Engineering  
 Pohang Institute of Science and Technology  
 Pohang P.O. Box 125, 790-600, KOREA

**ABSTRACT:** The POSTECH Hand adopting coupled tendon driven technique with planar two fingers is developed. The hand is designed to emulate principal motions of the human hand which has two and three joints respectively. Its kinematic parameters are determined through a parameter optimizing technique to aim at improving the isotropy of fingertip motions with new criterion functions of design. For the control of the hand, tension and torque control algorithms are developed. Based on the virtual stiffness concept, we develop the stiffness control method of a grasped object with redundant finger mechanism and investigate experimentally.

### 1 Introduction

The usefulness of multi-fingered robot hands can be easily found in robot applications which requires contact works. On the contrary, the design and control problems concerning kinematics, actuators, sensors, transmissions and control methodologies have limited the feasibility and applicability of the multi-fingered hands.

Kinematic issues are the fundamental step toward the design of multi-fingered robot hand. The selection of the structure and phalangeal length are the basics to be determined. In robot hands, actuator units can not be directly installed at joints due to spatial restrictions. They are normally put at the separated places and the power is delivered to the joint through intermediate transmissions such as tendon, belt, pulley or sheath[2, 4-6, 10, 12, 13]. The tendon actuating means are classified as three groups according to the configuration of tendon and actuator: they are  $N$  type[3-4],  $N + 1$  type[1] and  $2N$  types[2, 4], where the  $N$  represents the number of tendons to drive a joint. The control problem of tendon driven system is how to overcome the frictions and non-linearities caused by the intermediate transmissions. The previous works do not seem to be well investigated on this point. In other groups, the mechanisms to positively use interferences or couplings between tendons are proposed[1, 4]. They actively control the bias tensions but make the control system complicated.

In this paper, we present the human-like hand which has the thumb and index finger to emulate the princi-

pal motions of the human hand. Based on the determined hand model, the kinematic parameters are obtained through optimization technique. The hand adopts  $2N$  type coupled tendon driven method, which satisfies the requirement that overall hand system should be as small as possible. As the couplings of tendon let us use small powered motors in spite of the number of actuators, the size of system package can be reduced. In the low level control issues, the tension and torque controller is developed and its performances are experimentally investigated. Finally, we describes the stiffness control method of the grasped object. A stiffness controller for the redundant finger is devised and applied for the POSTECH Hand.

### 2 Kinematic Design

We propose criterion functions of design satisfying the globally specified isotropy, namely *Cooperative Weighted Workspace* and *Cooperative Average Isotropy*[6]. In the finger, the accuracy of static force exertion and directional evenness are the most important properties, which is represented by *isotropy*. The two criterion function of design evaluate the isotropy globally, which are based on the local measure of isotropy. The measure of isotropy  $\Delta$  is defines as follows:

$$M = \det(\mathbf{J}\mathbf{J}^T)^{1/m}, \quad (1)$$

$$\Psi = \text{trace}(\mathbf{J}\mathbf{J}^T) / m, \quad (2)$$

$$\Delta = \frac{M}{\Psi}, \quad (3)$$

where  $m$  is the number of joint and  $\mathbf{J}$  is the finger Jacobian. Mathematically,  $M$  is a *geometric mean* of eigenvalues of  $\mathbf{J}\mathbf{J}^T$  and  $\Psi$  represents the *arithmetic mean* of eigenvalues of  $\mathbf{J}\mathbf{J}^T$ . The measure of isotropy has an upper bound of 1 and lower bound 0. The local measure of isotropy  $\Delta$  is expanded to the criterion function of cooperative fingers, namely *Cooperative Weighted Workspace* and *Cooperative Average Isotropy*. The *Cooperative Weighted Workspace* is defined as:

$$W_c(\Delta) = \int_{R_c} \Delta_1 \cdot \Delta_2 \cdots \Delta_p \, dV, \quad (4)$$

where  $R_c = R_1 \cap R_2 \cap \dots \cap R_p$  and  $p$  denotes the number of fingers and  $\Delta_1 \cdot \Delta_2 \cdot \dots \cdot \Delta_p$  is the product of isotropy of each finger.

Also, the cooperative average dexterity can be defined similarly.

$$A_c(\Delta) = \frac{\int_{R_c} \Delta_1 \cdot \Delta_2 \cdot \dots \cdot \Delta_p dV}{\int_{R_c} dV} . \quad (5)$$

As the measure of isotropy is bounded from 0 to 1, the product of isotropy is bounded from 0 to 1. These measures may be used for evaluating cooperative capability of multi-fingered robot hand and can be used as criterion functions of design aiming at both of dexterity and workspace.

The model of two fingered hand is as shown in Fig. 1 and the design problems can be formulated as follows:

- Find six design parameters  $p_{b2} - p_{b1}$ ,  $L_1 \in \mathbb{R}^2$ ,  $L_2 \in \mathbb{R}^3$  where  $p_{b1}$   $p_{b2}$  are the base positions of each finger and  $L_1$ ,  $L_2$  are the concatenated vector of link length.
- Given  $\theta_{1min} \leq \theta_1 \leq \theta_{1max}$   
 $\theta_{2min} \leq \theta_2 \leq \theta_{2max}$   
where  $\theta_1$  means index joint angle and  $\theta_2$  means thumb joint angle.
- max  $W_c(\Delta)$  or  $A_c(\Delta)$

The formulated problem is solved using *Parameter Optimization Technique* and Table 1 includes the obtained dimensions of the hand.

Table 1: Dimensions of the POSTECH Hand

$L_{11}$	87.5
$L_{12}$	85
$p_{b2} - p_{b1}$	97
$L_{21}$	106
$L_{22}$	65
$L_{23}$	65

where the units are *mm*.

### 3 System Configuration

The 2N type tendon driven mechanism has several advantages but the control system becomes complicated. The POSTECH Hand is asymmetrically configured as a planar structure shown in Fig. 2. Among the two kinds of tendon routing methods[4], our system adopts symmetrical tendon routing( type I ), which shows even performance in extension and flexion. Tensions are measured by two cantilever beam element at the position as near as the drive joint which helps reduce the nonlinear effects of friction in transmission system. Instead of a specially designed torque sensor such as TDT sensor[8], we

use the reconstructed torque by tension measurements, which shows similar effects in torque feedback control. Ten torque controlled DC servo motors with harmonic reducer( rated torque 1.4Nm, torque constant 2.1Nm/A, and rated speed 60 rpm including harmonic reduction gear of 50:1 ) are used to actuate the tendons.

The overall hardware system are as illustrated in Figs. 3. All the controllers are implemented discretely. The hardware is composed of two target computers( Motorola MC68030 CPU single board computer ) in a VME-bus card cage, and host computer SPARC workstation. It has a D/A converter with 16 channels and a A/D converter with differential 16 channels. Motor positions are sensed by the 500 PPR incremental encoder which is used to generate velocity feedback. We directly measure the joint positions by potentiometers( 10 k $\Omega$ /turn ), which is very important in establishing stiffness controller[3]. The servo rate for each tendon tension controller is 360Hz and torque control or high level control loop runs at 80Hz. All the control programs are written in C language and a few 68030 assembly code. They are developed on a workstation in UNIX environment using a commercial realtime software development tool of VRTXvelocity[14].

### 4 Tension and Torque Control

Motor torque command is generated proportional to tendon tension error and velocity feedback is added to give stable motor torque control. The frictions at reducer, tendon, pulley and motors are compensated by the integral feedback with feedforward friction compensation. Also, lead compensator is added to remove sluggish system behavior. The actuator torque is computed by

$$\tau = r \cdot (K_T(f_d - f_m) + f_d + K_I \int (f_d - f_m) dt) (6) + K_D(\dot{\theta}_d - \dot{\theta}_m) + \text{sign}(\dot{\theta}_m) \cdot V_f + \tau_{lead} .$$

where,

- $f_d$  : desired tension
- $f_m$  : measured tension
- $r$  : pulley radius
- $\dot{\theta}_d$  : desired motor velocity
- $\dot{\theta}_m$  : measured motor velocity
- $K_T$  : tension force gain
- $K_I$  : tension integral gain
- $K_D$  : velocity feedback gain
- $V_f$  : motor static friction voltage
- $\tau$  : actuator torque command
- $\tau_{lead}$  : torque from lead compensator .

Joint torque controller is composed of PI and feedforward torque. It is reconstructed by measured tension according to the tension and torque relation( it is formulated in following Eq. (9) ) and the joint torque feedback control is accomplished. The joint torque command can

be written by

$$\boldsymbol{\tau}_m = \boldsymbol{D}\boldsymbol{T}, \quad (7)$$

$$\boldsymbol{\tau}_{cmd} = \boldsymbol{\tau}_d + \boldsymbol{K}_t(\boldsymbol{\tau}_d - \boldsymbol{\tau}_m) + \boldsymbol{K}_i \int (\boldsymbol{\tau}_d - \boldsymbol{\tau}_m) dt, \quad (8)$$

where,

$\boldsymbol{\tau}_m$	: measured joint torque
$\boldsymbol{\tau}_{cmd}$	: joint torque command
$\boldsymbol{K}_t$	: torque proportional gain
$\boldsymbol{K}_i$	: torque integral gain
$\boldsymbol{D}$	: coefficient matrix of tension and torque
$\boldsymbol{T}$	: measured tension vector.

Joint torques are exerted by coordinating a set of tension controllers. Although the coordination of tension is a kind of redundancy resolution problem, in actual implementations, we need a fast and simple algorithm. The relationship between the joint torque  $\boldsymbol{\tau}$  and tension  $\boldsymbol{f}$  is represented in a matrix form as

$$\boldsymbol{\tau}_{cmd} = \boldsymbol{D}\boldsymbol{f}, \quad (9)$$

where

$\boldsymbol{\tau}_{cmd} = \{\tau_1 \dots \tau_n\}^T$  and  $\boldsymbol{f} = \{f_1 \dots f_{2n}\}^T$  are the joint torque and tendon tension[4].  $\boldsymbol{D} \in \mathbb{R}^{n \times 2n}$  is the constant coefficient matrix whose elements consist of the pulley radius  $r$ . The matrix  $\boldsymbol{D}$  describes the geometric features of the coupled tendon driven mechanism and the index finger has the matrix  $\boldsymbol{D}$  as

$$\boldsymbol{D} = \begin{bmatrix} r & -r & -r & r & r & -r \\ 0 & 0 & r & -r & -r & r \\ 0 & 0 & 0 & 0 & r & -r \end{bmatrix} \quad (10)$$

By the principle of virtual work, the joint displacement  $\delta\boldsymbol{\theta}$  and tendon displacement  $\delta\boldsymbol{x}$  are related as

$$\delta\boldsymbol{x} = \boldsymbol{D}^T \delta\boldsymbol{\theta}. \quad (11)$$

A simplest way to implement the redundancy resolution problem can be written by

$$\boldsymbol{f} = \boldsymbol{D}^+ \boldsymbol{\tau}_{cmd} + [\boldsymbol{I} - \boldsymbol{D}^+ \boldsymbol{D}] \boldsymbol{f}_o, \quad (12)$$

where  $\boldsymbol{f}_o$  is arbitrary tension vector balanced internally and  $\boldsymbol{D}^+$  is the pseudoinverse of matrix  $\boldsymbol{D}$ , which is written by

$$\boldsymbol{D}^+ = \boldsymbol{D}^T (\boldsymbol{D}\boldsymbol{D}^T)^{-1}. \quad (13)$$

Because the tendon can only exerts traction forces, the pseudoinverse solution can not be applied to the tension control loop directly. The tractional force constraint yields,

$$\boldsymbol{f} \geq \boldsymbol{f}_{MIN} > 0, \quad (14)$$

where  $\boldsymbol{f}_{MIN}$  is the minimum traction forces for each tendon. In our hand, there is no torque variation if we in-

crease all the tensions equally due to the symmetrical tendon routing. Therefore, we can develop an algorithm to get tensions satisfying the Eq. (9) and constraints simultaneously. It is coded as follows:

```

compute  $\boldsymbol{f} = \boldsymbol{D}^+ \boldsymbol{\tau}_{cmd}$ 
Find  $f_{imin}$  where  $i = 0, \dots, 2n$ 
for  $j = 0$  to  $2n$  {
If  $f_{imin} < f_{MIN}$ 
 $f_j = f_j + (f_{MIN} - f_{imin})$ 
Else  $f_j = f_j$ 
} .

```

## 5 Fingertip Stiffness Control

Under the virtual stiffness concept, the fingertip can be replaced by a set of generalized virtual springs  $\boldsymbol{K}_v$  (in planer case,  $\boldsymbol{K}_v \in \mathbb{R}^{2 \times 2}$ )[7, 11]. The problem is how to control the joint servo stiffness to generate a desired virtual fingertip stiffness. In the case of the thumb, joint stiffness can be obtained via *Active Stiffness Control*[1], where the virtual fingertip stiffness  $\boldsymbol{K}_{iv}$  is mapped to the joint as follows:

$$\boldsymbol{K}_{i\theta_s} = \boldsymbol{J}_{i\theta}^T \boldsymbol{K}_{iv} \boldsymbol{J}_{i\theta}. \quad (15)$$

where

$\boldsymbol{K}_{i\theta_s}$ :	joint stiffness of the thumb
$\boldsymbol{K}_{iv}$ :	fingertip virtual stiffness of the thumb
$\boldsymbol{J}_{i\theta}$ :	finger Jacobian of the thumb.

However, the index finger which has a redundant degree of freedom can not be controlled by this method. The *Orthogonal Decomposition Control* can overcome this problem by actively controlling the null stiffness of the redundant finger[13]. When the virtual fingertip stiffness of the index finger  $\boldsymbol{K}_{iv}$  is given, there are infinite number of index joint stiffness  $\boldsymbol{K}_{i\theta_s}$  satisfying the given virtual stiffness. For a positive definite stiffness  $\boldsymbol{K}_{iv}$ , if we apply active stiffness control law,  $\boldsymbol{K}_{i\theta_s}$  is always singular when there is a redundancy. That is,  $\boldsymbol{K}_{i\theta_s}$  is positive semi-definite and has the same number of zero eigenvalues as the degree of redundancy. The positive semidefinite stiffness matrix causes the instability of the finger configuration. The problem, therefore, is to derive a non-singular  $\boldsymbol{K}_{i\theta_s} \in \mathbb{R}^{3 \times 3}$  satisfying the given symmetric positive definite virtual stiffness  $\boldsymbol{K}_{iv} \in \mathbb{R}^{2 \times 2}$ .

Let the positive semidefinite joint stiffness matrix  $\tilde{\boldsymbol{K}}_{i\theta_s}$  which is obtained by active stiffness control. By the use of similarity transform, we can obtain a diagonal matrix  $\boldsymbol{A}_p$  as follows.

$$\boldsymbol{A}_p = \boldsymbol{M}^T \tilde{\boldsymbol{K}}_{i\theta_s} \boldsymbol{M} \quad (16)$$

$$= \begin{bmatrix} \lambda_1 & 0 & 0 \\ 0 & \lambda_2 & 0 \\ 0 & 0 & \lambda_3 \end{bmatrix} \quad (17)$$

where the columns of the orthogonal matrix  $M(M^{-1} = M^T)$  are the eigenvectors corresponding to eigenvalues  $\lambda_1$ ,  $\lambda_2$  and  $\lambda_3$  of  $\tilde{K}_{i\theta s}$ , respectively and

$$\lambda_1 \geq \lambda_2 \geq \lambda_3 = 0 \quad (18)$$

If we shift  $\lambda_3$  to an arbitrary positive value, the orthogonal matrix  $M$  remains the same, which enables us to construct a new non-singular joint stiffness matrix  $K_{i\theta s}$ . How to determine  $\lambda_3$  is important in the view of the grasp stability as the additional stiffness induced from internal forces affects the effective overall joint stiffness of the finger[7]. The safest way to preserve the grasp stability is to take mean value of the other eigenvalue as follows.

$$\lambda_3 = \frac{\lambda_1 + \lambda_2}{2} \quad (19)$$

A new positive definite stiffness matrix  $K_\theta$  is defined as

$$A = A_p + A_h \quad (20)$$

$$= M^T \tilde{K}_{i\theta s} M + \lambda_3 I_3 \quad (21)$$

where

$$A_h = \lambda_3 I_3 \quad (22)$$

and

$$I_3 = \begin{bmatrix} 0 & 0 & 0 \\ 0 & 0 & 0 \\ 0 & 0 & 1 \end{bmatrix} \quad (23)$$

Therefore, the matrix  $A_h$  is always orthogonal to the matrix  $A_p$ . The new positive definite joint stiffness matrix  $K_\theta$  is obtained by

$$K_\theta = M A M^T \quad (24)$$

$$= J_{i\theta}^T K_{i\theta} J_{i\theta} + \lambda_3 S \quad (25)$$

$$= K_{i\theta p} + K_{i\theta h} \quad (26)$$

where

$$S = M I_3 M^T \quad (27)$$

$$K_{i\theta p} = J_{i\theta}^T K_{i\theta} J_{i\theta} \quad (28)$$

$$K_{i\theta h} = \lambda_3 S \quad (29)$$

The matrix  $S$  enables us to assign a new nonzero eigenvalue  $\lambda_3$  in the direction perpendicular to the hyperplane in which  $K_{i\theta p}$  lies. The  $\lambda_3$  determines the magnitude of the null motion stiffness in the direction of redundancy, which correspond to the last eigenvector of matrix  $M$ .

Using this scheme, we can control the index finger and Fig. 4 shows the fingertip stiffness control performance of the index finger. Here, the virtual displacement means the commanded displacement of the fingertip. In the experiment, the fingertip contacts on a single axis force sensor. Though there can be no displacement, due to the fingertip stiffness effect, the force sensor reads forces as much as the virtual displacement times fingertip stiffness.

## 6 Object Stiffness Control

The ultimate goal of stiffness control of a hand is to generate desired stiffness for a grasped object at a given object coordinate. First, we assume that the contact is a hard point contact with friction and thus, the contact point is not changed. Also, the grasp force is assumed to be determined by an adequate contact force distribution algorithm. According to the previous works[7, 10], The object stiffness is related to the fingertip stiffness as:

$$K_o = \sum_{i=1}^m J_{oi}^{vT} K_{vi} J_{oi}^v + \Delta K_o, \quad (30)$$

where

$K_o$	: object stiffness
$J_{oi}^v$	: Jacobian from object to fingertip
$K_{vi}$	: fingertip stiffness of $i$ -th finger
$m$	: number of fingers

Also,  $\Delta K_o$  is an additional stiffness caused by grasping forces. The additional stiffness contributes only to the rotational stiffness and it should be considered in stiffness control because it may cause the object unstable as the grasp forces increase. As it is not controllable stiffness assuming that the fingertip forces are predetermined, the problem is how to control the fingertip virtual stiffness, which is another topic to be discussed. In this paper, we follow the fingertip stiffness synthesis procedure proposed by Kaneko[11]. The proposed controllers from tendon level to object stiffness level are constructed hierarchically and summarized as shown in Fig. 5.

Through the experiments, we demonstrate contact tasks can be accomplished successfully. The object is commanded to track a given circular trajectory of a 20mm radius and to remove the inertia effect, a quasi-static motion is commanded. The grasped object encounters a rigid wall( actually, it is a single axis force sensor ) at a given position as in Fig. 6. When the object contacts with the wall, it behaves like a spring and comes to exert the force proportional to the depressed desired path. The stiffness of the object is given by

$$K_o = \begin{bmatrix} 500 & 0 & 0 \\ 0 & 500 & 0 \\ 0 & 0 & 10 \end{bmatrix} \quad (31)$$

where the unit of translation stiffness is  $N/m$  and that of rotational stiffness is  $N/m/radian$ . The performance of contact motion can be found in Figs. 7 and 8. We can find the depressed path and the measured forces are proportional and moreover, approximately equal to the given object stiffness.

## 7 Conclusion

Design and control procedures of the POSTECH Hand

adopting coupled tendon driven method is developed and experimentally verified. We propose the global criterion function of design, namely *Cooperative Weighted Workspace and Cooperative Average Dexterity*. Using these measures, we determine the kinematic parameters of the hand. The hand controller is constructed by hierarchical subcontrollers from the tension to the object level. Also, a new redundant finger controller called the *Orthogonal Decomposition Control*, is proposed to overcome the limit of conventional stiffness controller. Through experiments, we demonstrate that the proposed hardware configuration and the control methods are feasible to control general types of multi-fingered hand including redundant joints.

## References

- [1] J. K. Salisbury and J. J. Craig, "Articulated Hands: Force Control and Kinematic Issues," *Int. J. Robotics Research*, vol. 1, no. 1, pp. 4-17, 1982.
- [2] S. C. Jacobson, D. F. Wood, and K. B. Biggers, "The Utah/MIT Dextrous Hand - Work in Progress," *Int. J. Robotics Research*, vol. 3, no. 4, pp. 1520-1532, 1984.
- [3] N. Imamura, M. Kaneko, K. Yokoi, and K. Tanie, "Development of a Two-fingered Robot Hand with Compliance Adjustment Capability", *Proc. Japan-U.S.A Symposium on Flexible Automation, ISCIE*, Kyoto, JAPAN, pp. 997-1004, 1990.
- [4] S. Hirose and S. Ma, "Coupled Tendon-driven Multi-joint Manipulator", *Proc. of the IEEE Conf. on Robotics and Automation*, Sacramento, CA, pp. 1268-1275, 1991.
- [5] T. Iberal, "The Nature of Human Prehension: Three Dextrous Hands in One," *Proc. of the IEEE Conf. on Robotics and Automation*, Raleigh, NC, pp. 396-401, 1987.
- [6] H. R. Choi, W. S. Yum, W. K. Chung, and Y. Youm, "New Design Concepts of Anthropomorphic Multi-fingered Hands", *Proc. of ITOMM-jc Int. Symp. Theory Machines and Mechanisms*, Nagoya, Japan, pp. 318-323, 1992.
- [7] H. R. Choi, W. K. Chung and Y. Youm, "Stiffness Analysis of Multi-fingered Robot Hand," *Proc. IEEE/RSJ Int. Conf. on Intelligent Robots and Systems*, Yokohama, Japan, pp. 883-888, 1993.
- [8] M. Kaneko, K. Yokoi, and K. Tanie, "On a New Torque Sensor for Tendon Drive Fingers," *Trans. IEEE Robotics and Automation*, vol. 6, no. 4, pp. 501-507, 1990.
- [9] H. Mackawa, M. Kaneko, K. Yokoi, K. Tanie, and N. Inamura, "Grasp Control for a Multifingered Hand with Kinematic Redundancy", *JSME International Journal Series III*, vol. 33, no. 4, pp. 546-552, 1990.
- [10] V. Nguyen, "Constructing Stable Grasps," *Int. J. Robotics Research*, vol. 1, no. 1, pp. 26-37, 1989.
- [11] M. Kaneko M., N. Imamura N., K. Yokoi, and K. Tanie, "A Realization of Stable Grasp Based on Virtual Stiffness Model by Robot Fingers," *Proc. IEEE Int. Workshop on Advanced Motion Control*, Yokohama, Japan, pp. 156-163, 1983.
- [12] J. O. Kim and P. Khosla, "Dexterity Measures for Design and Control of Manipulator," *Proc. IEEE/RSJ Int. Workshop on Intelligent Robots and Systems*, Osaka, Japan, pp. 758-763, 1991.
- [13] J. O. Kim, P. Khosla and W. K. Chung, "Static Modeling and Control of Redundant Manipulators," *Robotics & Computer-Integrated Manufacturing*, vol. 9, no. 2, pp. 145-157, 1992.
- [14] Ready Systems Inc., *Manual of VRTXvelocity, realtime O/S*, 1991.

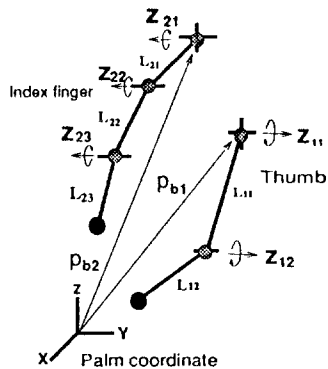


Figure 1: Two fingered hand model

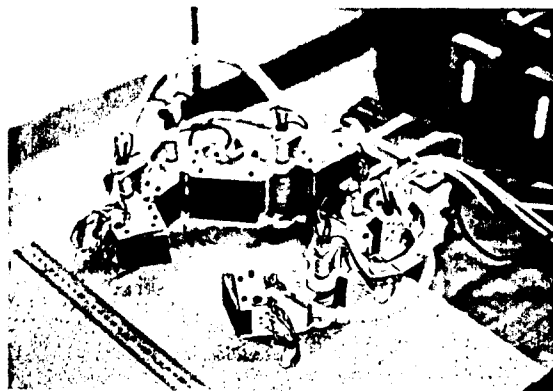


Figure 2: POSTECH two-fingered robot hand

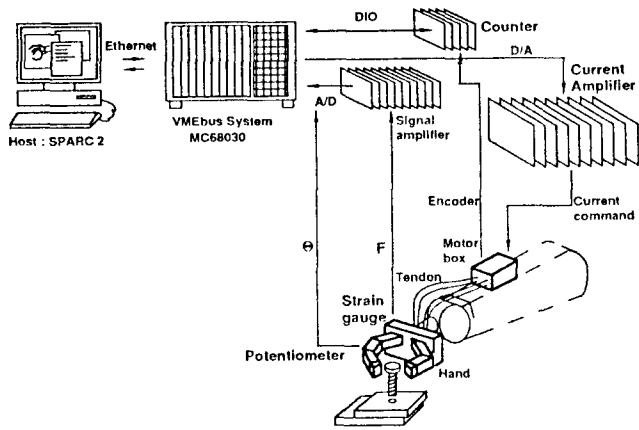


Figure 3: Hardware architecture

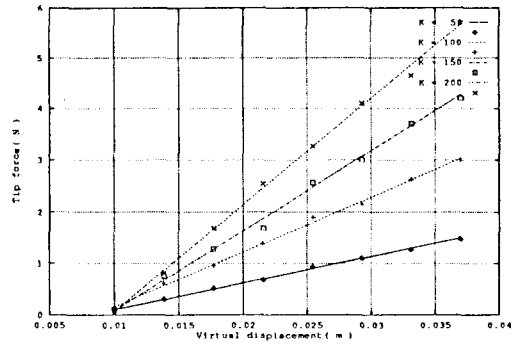


Figure 4: Fingertip stiffness control performance

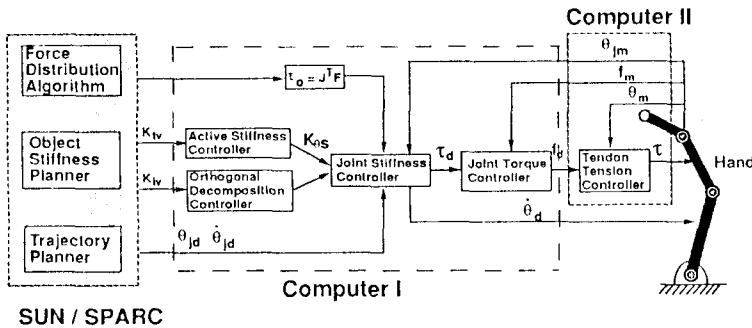


Figure 5: Hand controller

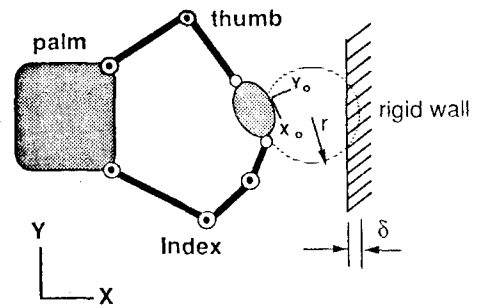


Figure 6: Experiment schematic

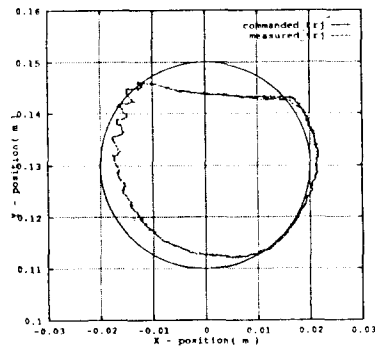


Figure 7: Constrained motion trajectory of the grasped object

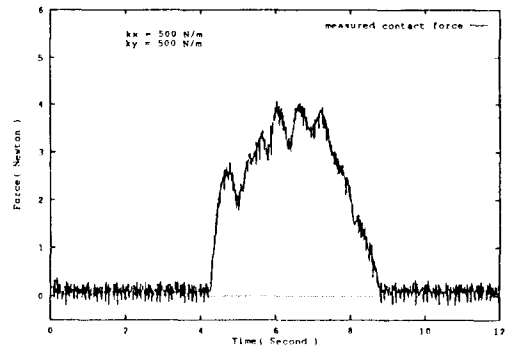


Figure 8: Measured contact force in constrained motion